JOURNAL OF APPLIED ELECTROCHEMISTRY **25** (1995) 155–165

Cathodic reduction of hypochlorite during reduction of dilute sodium chloride solution

M. RUDOLF, I. ROUSAR, J. KRYSA

Department of Inorganic Technology, Institute of Chemical Technology, 166 28 Prague 6, Czech Republic

Received 19 January 1994; revised 6 May 1994

Sodium chloride solutions of concentration 15 and 30 g dm^{-3} were electrolysed in a flow-through electrolyser with a titanium/TiO_2/RuO_2 anode at current densities 1059–4237 A m^{-2}. The current yield for the reduction of hypochlorite on a stainless steel cathode was found to be 13–32% at 7 g dm^{-3} NaClO, in agreement with that calculated on the basis of the Stephan–Vogt theory. Migration of ions was taken into account, the diameter of hydrogen bubbles was set equal to 0.04 mm and the coverage of the electrode with the bubbles was estimated as $\theta = 0.897$. The results of calculations show that the reduction rate of hypochlorite at low NaCl concentrations is lowered by migration. Literature data for the reduction of hypochlorite are in accord with the current yield calculated on the basis of the Stephan–Vogt theory using $\theta = 0.787$ and $\theta = 0.949$.

List of symbols

C_i^0	concentration of species i in the bulk (mol m^{-3})
C_i^s	concentration of species i at the cathode surface (mol m^{-3})
d_B	bubble diameter (m)
D_e	equivalent diameter (characteristic dimension) (m)
D_i	diffusion coefficient of species i (m^2 s^{-1})
f_G	gas evolution efficiency
F	Faraday constant (96 487 C mol^{-1})
j	total current density (A m^{-2})
j_B	current density for gas evolution (A m^{-2})
$j_{c,lim}$	limiting current density for cathodic reduction of ClO^- (A m^{-2})
$j_{c,r}$	critical current density (A m^{-2})
L	length of electrode (m)
M	migration correction factor
n_B	number of electrons exchanged in gas evolution
n_{ClO^-}	number of electrons exchanged in reduction of ClO^-
N_i	flux of species i (mol m^{-2} s^{-1})
Q	charge passed (C)
P_t	total gas pressure (Pa)
Re	Reynolds number (Equation 14)
Re_B	Reynolds number (Equation 17)
Sc	Schmidt number (Equation 13)
Sh	Sherwood number (Equation 12)
Sh_B	Sherwood number (Equation 15)
T	absolute temperature (K)
u_i	mobility of ion i (m^2 s^{-1} V^{-1})
v_B	fictitions linear velocity of gas formation (m s^{-1})
v_{el}	rate of electrolyte flow (m s^{-1})
V	volume of the electrolyte in the system (m^3)
V_{H_2}	content of hydrogen in gas phase (%)
V_{O_2}	content of oxygen in gas phase (%)
y_i	current yield (differential) for production of species i (%)
y_r	current yield (differential) for reduction of ClO^- and ClO_3^- (%)
$y_{ClO^-,r}$	current yield (differential) for reduction of ClO^- (%)
Y_i	integral current yield for production of species i (%)
z_i	charge number of ion i

Greek symbols

δ	thickness of Nernst diffusion layer (m)
δ_C	thickness of convective diffusion layer (m)
δ_B	thickness of diffusion layer controlled by gas evolution (m)
ν	dynamic viscosity (m^2 s^{-1})
τ	time (s)
θ	coverage of electrode surface with gas bubbles
ϕ	Galvani potential (V)
Φ	correction function (Equation 11)

1. Introduction

Electrolysis of dilute NaCl solution is used for the preparation of hypochlorite solutions for disinfection of potable water [1, 2]. Reduction of the hypochlorite on the cathode, however, constitutes a serious problem, causing a 15–65% drop in the current yield for hypochlorite production. In contrast to other papers [1, 3, 4] the aim of the present study was to perform experiments under defined hydrodynamic conditions. The data thus obtained enable a comparison of the measured current yields with those based on the theory [5, 6].

0021-891X

2. Theory

2.1. *Reactions during electrolytic preparation of hypochloride*

The main anodic reaction is the formation of chlorine

$$2Cl^- = Cl_2 + 2e^- \quad (1)$$

The side reaction is the evolution of oxygen according to either

$$4OH^- = O_2 + 2H_2O + 4e^- \quad (2)$$

or by the Foerster reaction

$$6ClO^- + 3H_2O = 2ClO_3^- + 6H^+ + 4Cl^- + 1.5O_2 + 6e^- \quad (3)$$

The main cathodic reaction is the evolution of hydrogen

$$2H_2O + 2e^- = 2OH^- + H_2 \quad (4)$$

and the side reactions are the reduction of hypochlorite and chlorate

$$ClO^- + H_2O + 2e^- = Cl^- + 2OH^- \quad (5)$$

$$ClO_3^- + 3H_2O + 6e^- = 6OH^- + Cl^- \quad (6)$$

The dissolved chlorine in the weakly alkaline bulk solution undergoes hydrolysis

$$Cl_2 + 2OH^- = ClO^- + Cl^- + H_2O \quad (7)$$

and the ClO^- ions may react chemically to give chlorate

$$2HClO + ClO^- = ClO_3^- + 2H^+ + 2Cl^- \quad (8)$$

Decomposition reactions lead to the formation of oxygen according to

$$HClO = H^+ + Cl^- + \tfrac{1}{2}O_2 \quad (9a)$$

$$ClO^- = Cl^- + \tfrac{1}{2}O_2 \quad (9b)$$

Reaction 7 suggests that nearly all the chlorine formed at the anode is converted to hypochlorite ions in sufficiently alkaline medium. The concentration of molecular chlorine, and hence its partial pressure above the solution is negligible.

According to Hardee and Mitchell [7], the decomposition of hypochlorite by Reactions 9(a) and (b) is negligible at NaClO concentrations up to $10\,g\,dm^{-3}$ at 20° C in solutions of common purity. Bennett [4] and Krstajić [2] consider the rate of chlorate formation by Reaction 8 at pH 8.3–9.0 negligible at low temperatures (~ 20° C). According to Hammar and Wranglen [3], the current yield of the cathodic reduction of hypochlorite is directly proportional to its concentration and inversely proportional to current density. It increases with temperature and decreases with rising NaCl concentration. The authors [3] discussed these findings on the assumption that the reduction of hypochlorite is controlled by its convective diffusion to the cathode surface.

2.2. *Calculation of the diffusion layer thickness*

When the transport of mass (ions) near the cathode is only controlled by forced convection, the mass transfer coefficient or the thickness of the diffusion layer at the cathode wall of a flow-through channel can be calculated as follows [8]:

$$Sh = 0.023\, Re^{0.8} Sc^{1/3} \quad (10)$$

in the turbulent region ($Re > 2300$), and

$$Sh = 1.85\left(Re\, Sc \frac{D_e}{L}\right)^{1/3} \Phi \quad (11)$$

in the laminar region ($Re < 2300$). The dimensionless numbers are defined as listed at the outset.

$$Sh = \frac{D_e}{\delta_C} \quad (12)$$

$$Sc = \frac{\nu}{D_{ClO^-}} \quad (13)$$

$$Re = \frac{\nu_{el} D_e}{\nu} \quad (14)$$

The function Φ is equal to unity when the interelectrode distance is small with respect to the channel width. When the transport of mass (ClO^- ions) to the cathode is controlled by the cathodic evolution of hydrogen, the following equation [5] applies:

$$Sh_B = 0.93\, Re_B^{0.5} Sc^{0.487} \left[\frac{\Theta^{0.25}(1-\Theta^{0.5})^{0.5}}{\Theta_1^{0.25}(1-\Theta_1^{0.5})^{0.5}}\right] \quad (15a)$$

or for $0.15 \langle \theta_1 \rangle 0.4$ Equation 15(a) can be rewritten [9, 10] as

$$Sh_B = 1.89\, Re_B^{0.5} Sc^{0.487} [\Theta^{0.5}(1-\Theta^{0.5})]^{0.5} \quad (15b)$$

where

$$Sh_B = \frac{d_B}{\delta_B} \quad (16)$$

$$Re_B = \frac{\nu_B d_B}{\nu} f_G \quad (17)$$

$$\nu_B = \frac{-j_B RT}{n_B F P_t} \quad (18)$$

θ is the coverage of the electrode surface with bubbles and θ_1 is in the range of $0.15 \langle \theta_1 \rangle 0.4$. The recommended value for the diameter of hydrogen bubbles in alkaline solution is $d_{B1} = 0.04$ mm. The gas evolution efficiency, f_G [10, 11] for $\theta = 0.8$ is $f_G = 0.98$ and for $\theta \geqslant 0.8$ f_G is approximately equal to 1.

When the mass transfer of (ClO^- ions) is controlled both by forced convection and by gas evolution, the following equations [6] apply:

$$\frac{1}{\delta} = \left[\left(\frac{1}{\delta_C}\right)^2 + \left(\frac{1}{\delta_B}\right)^2\right]^{1/2} \quad (19)$$

and

$$\frac{j_{c,lim}}{n_{ClO^-} F} = -C^0_{ClO^-} \frac{D_{ClO^-}}{\delta} M \quad (20)$$

where M is a correction for migration, which approaches 1 with increasing concentration of the base electrolyte; otherwise it is less than 1 for the studied system.

It follows from Equation 15(a) that the thickness of the Nernst diffusion layer depends on both the bubble diameter, d_B, and the coverage, θ. For two cases with the same thickness of the Nernst diffusion layer and constant Schmidt number, but different bubble diameters d_B and different coverages θ, we have

$$\frac{d_{B1}}{\Theta_1^{0.5}(1-\Theta_1^{0.5})} = \frac{d_{B2}}{\Theta_2^{0.5}(1-\Theta_2^{0.5})} \tag{21}$$

This relation is important for elucidation of the influence of changing d_B and θ in Equation 15(a). Stephan and Vogt [5] recommend use of the values $d_{B1} = 0.04\,\text{mm}$ and $\theta_1 = 0.25$ for hydrogen in alkaline solutions. From Equation 21 it follows that the bubble diameter $d_{B2} = 0.2\,\text{mm}$ and coverage $\theta_2 = 0.728$ satisfy the same experimental data.

The effect of changing coverage during changing current density can be seen from Fig. 4 in [5]. The scatter of experimental data is considerable and can be attributed to the fact that the changing current density causes changes in the electrode coverage with bubbles and in the bubble diameters.

2.3. *Calculation of the current yield for cathodic reduction of hypochlorite without the effect of migration*

At the limiting current density, the concentration of ClO^- ions at the cathode surface is to zero and the reduction rate is controlled by transport from the bulk solution to the electrode surface. If migration of ClO^- ions can be neglected, their flux normal to the cathode is given by

$$N_{ClO^-} = \frac{j_{c,lim}}{n_{ClO^-}F} = C^0_{ClO^-}\frac{D_{ClO^-}}{\delta} \tag{22}$$

The total current density is equal to the sum of the partial current densities for Reaction 4, j_B, and for reduction of ClO^-, $j_{c,lim}$:

$$j = j_{c,lim} + j_B \tag{23}$$

The current yield for reduction of ClO^- ions, $y_{ClO^-,r}$ is given as

$$y_{ClO^-,r} = \frac{j_{c,lim}}{j} \times 100 \tag{24}$$

where j denotes total current density.

2.4. *Calculation of the current yield for cathodic reduction of hypochlorite with the effect of migration*

The flux of ions is, in general, given by diffusion, migration and convection. The x component of the flux is given as

$$N_i = -D_i\left(\frac{dC_i}{dx}\right) - u_iC_i\left(\frac{d\phi}{dx}\right) + \nu_xC_i \qquad i = 1,\ldots,N \tag{25}$$

The concentrations satisfy the condition of electroneutrality

$$\sum C_iz_i = 0 \tag{26}$$

From these two equations, in the steady state $((\delta C_i/\delta\tau) = 0)$ and in the Nernst boundary layer (i.e. for $v_x = 0$) [12], we obtain:

$$-D_i\left(\frac{d^2C_i}{dx^2}\right) - u_i\left(\frac{dC_i}{dx}\right)\left(\frac{d\phi}{dx}\right) - u_iC_i\left(\frac{d^2\phi}{dx^2}\right) = 0 \qquad i = 1,\ldots,N \tag{27}$$

The following expression for the potential gradient can be derived [14] from Equation 27:

$$\frac{d\phi}{dx} = \frac{-\frac{j}{F} - \sum_{i=1}^{N-1}(D_i - D_N)z_i\frac{dC_i}{dx}}{\sum_{i=1}^{N-1} z_iC_i(u_i - u_N)} \tag{28}$$

and an analogous expression can be obtained for the second derivative

$$\frac{d^2\phi}{dx^2} = \frac{\sum_{i=1}^{N-1}((u_i/D_i) - (u_N/D_N))z_i\frac{dC_i}{dx}}{\sum_{i=1}^{N-1} z_iC_i((u_i/D_i) - (u_N/D_N))} \tag{29}$$

In the present case (in the weakly alkaline region, pH 9.5), we consider the limiting current due to the reduction of ClO^- and ClO_3^- ions. The boundary conditions at the cathode surface are

$$C^s_{ClO^-} = 0 \tag{30}$$

$$C^s_{ClO_3^-} = 0 \tag{31}$$

$$N^s_{ClO^-} + N^s_{ClO_3^-} = -N^s_{Cl^-} \tag{32}$$

$$\frac{j}{F} = -N^s_{OH^-} \tag{33}$$

The following subscripts refer to the ions: $1 = OH^-$, $2 = Cl^-$, $3 = ClO^-$, $4 = ClO_3^-$ and $5 = Na^+$. It is assumed that the bulk concentrations of the ions are known (from analysis and pH measurement). Subscript 's' refers to the interface.

Combining Equations 25, 30 and 31 with Equations 32 and 33, gives

$$-D_3\left[\frac{dC_3}{dx}\right]^s - D_4\left[\frac{dC_4}{dx}\right]^s = D_2\left[\frac{dC_2}{dx}\right]^s + u_2C_2^s\left[\frac{d\phi}{dx}\right]^s \tag{34}$$

and

$$\frac{j}{F} = D_1\left[\frac{dC_1}{dx}\right]^s + u_1C_1^s\left[\frac{d\phi}{dx}\right]^s \tag{35}$$

Multiplying Equation 34 by $z_2(u_2 - u_5)/u_2$ and Equation 35 by $z_1(u_1 - u_5)/u_1$ yields

$$\left[-\sum_{i=2}^{N-1} D_i \left[\frac{dC_i}{dx}\right]^s\right] \frac{z_2(u_2 - u_5)}{u_2} = z_2(u_2 - u_5)C_2^s \left[\frac{d\phi}{dx}\right]^s \quad (36)$$

$$\left[\frac{j}{F} - D_1 \left[\frac{dC_1}{dx}\right]^s\right] \frac{z_1(u_1 - u_5)}{u_1} = z_1(u_1 - u_5)C_1^s \left[\frac{d\phi}{dx}\right]^s \quad (37)$$

Introducing the potential gradient, Equation 28, into Equations 36 and 37, adding and using the boundary conditions $C_3^s = C_4^s = 0$ the following equation is obtained which involves the surface concentration gradients but not the concentration C_1^s and C_2^s:

$$\left[-\sum_{i=2}^{N-1} D_i \left[\frac{dC_i}{dx}\right]^s\right] \frac{z_2(u_2 - u_5)}{u_2} + \left[\frac{j}{F} - D_1 \left[\frac{dC_1}{dx}\right]^s\right] \times \frac{z_1(u_1 - u_5)}{u_1} = -\frac{j}{F} - \sum_{i=1}^{N-1} (D_i - D_N) \left[\frac{dC_i}{dx}\right]^s \quad (38)$$

From this equation the surface concentration gradient of OH^- ions ($i = 1$) can be expressed as

$$\left[\frac{dC_1}{dx}\right]^s = z_2 \left[-\sum_{i=2}^{N-1} D_i \left[\frac{dC_i}{dx}\right]^s \left[1 - \frac{u_5}{u_2}\right]\right] + \frac{j}{F}\left[z_1\left(\frac{u_5}{u_1} - 1\right) - 1\right] - \sum_{i=2}^{N-1} (D_i - D_N) z_i \left[\frac{dC_i}{dx}\right]^s \Bigg/ D_5(z_5 - z_1) \quad (39)$$

From Equations 34 and 35 the following relation between surface concentrations C_2^s and C_1^s is obtained:

$$C_2^s = \frac{-\sum_{i=2}^{N-1} D_i \left[\frac{dC_i}{dx}\right]^s}{\frac{j}{F} - D_1 \left[\frac{dC_1}{dx}\right]^s} \times \frac{u_1 C_1^s}{u_2} \quad (40)$$

Since the concentrations of all ions in the bulk phase are known and Equations 39 and 40 give constraints between surface concentrations of OH^- and Cl^- ions and their gradients, the system of second order differential equations of Equations 27–29 can be solved by iteration. To this end, the fourth-order Runge–Kutta–Merson method of numerical integration was used. The solution gives the fluxes of all ions under consideration and the distributions of concentration and Galvani potential in the Nernst boundary layer. The correction factor, M, for migration can then be calculated from the flux of ClO^- ions to the cathode surface and Equation 20.

The current yield with respect to reduction of hypochlorite, $y_{ClO^-,r}$, is defined as

$$y_{ClO^-,r} = \left|\frac{2N^s_{ClO^-}}{N^s_{OH^-}}\right| \times 100 \quad (41)$$

2.5. *Balance equations involving current yields*

The current yields with respect to ClO^- and ClO_3^- ions can be calculated from their concentrations, determined at the beginning and at the end of a given time interval. Balance calculations for processes in the electrolyser are based on these data and on gas analysis. Further we denote the current yield (differential) of species i as y_i; this is equal to the ratio of the charge consumed in production of species i to the total charge passed (in the differential period).

At the cathode, hydrogen is evolved by Reaction 4 (y_{H_2}), ClO^- and ClO_3^- ions are reduced by Reactions 5 and 6 (y_r). At the anode, chlorine is formed by Reaction 1 (y_{Cl_2}) and oxygen is evolved by Reactions 2 and 3 (y_{O_2}). The cathodic charge must equal the anodic one, hence

$$y_{H_2} + y_r = y_{Cl_2} + y_{O_2} \quad (42)$$

Chlorine formed at the anode is converted to hypochlorite by Reaction 7 (y'_{ClO^-}) and to chlorate by Reactions 3 and 8 ($y'_{ClO_3^-}$)

$$y_{Cl_2} = y'_{ClO^-} + y'_{ClO_3^-} \quad (43)$$

The amounts of ClO^- and ClO_3^- ions formed can be divided into those found analytically (y_{ClO^-} and $y_{ClO_3^-}$) and those reduced at the cathode (y_r) by Reactions 5 and 6:

$$y'_{ClO^-} + y'_{ClO_3^-} = y_{ClO^-} + y_{ClO_3^-} + y_r \quad (44)$$

Combining Equations 40 and 42 gives

$$y_{H_2} = y_{ClO^-} + y_{ClO_3^-} + y_{O_2} \quad (45)$$

From the equation of state of ideal gases and from Faraday's law (assuming ideal gas behaviour) the ratio of the current yields of oxygen and hydrogen is equal to twice the volume ratio of oxygen to hydrogen formed:

$$\frac{y_{O_2}}{y_{H_2}} = 2\frac{V_{O_2}}{V_{H_2}} \quad (46)$$

By introducing this result into Equation 45, the current yield of oxygen can be expressed as

$$y_{O_2} = \frac{y_{ClO^-} + y_{ClO_3^-}}{(0.5V_{O_2}/V_{H_2}) - 1} \quad (47)$$

$$y_r = 100 - y_{H_2} \quad (48)$$

It follows from Equations 42–48 that the current yields for cathodic reduction of ClO^- and ClO_3^- ions (y_r) can be found experimentally from the volume ratio of oxygen to hydrogen and from the values of y_{ClO^-} and $y_{ClO_3^-}$ found analytically. If the sum $y_{ClO^-} + y_{ClO_3^-}$ tends to zero the efficiency y_{O_2} tends to y_{H_2}.

3. Experimental details

3.1. *Apparatus*

The apparatus for production of sodium hypochlorite consisted of an electrolyser, source of d.c. current, thermostat (Labora, Prague), water spiral cooler, gas separator, Orsat device, Venturi tube with a U-

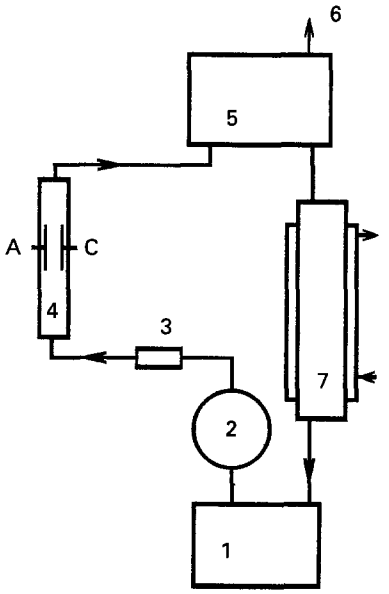

Fig. 1. Apparatus: (1) reservoir, (2) circulation pump, (3) Venturi tube and U-manometer, (4) electrolyser, (5) gas separator, (6) inlet to the Orsat devise, (7) spiral cooler, A = anode, C = cathode.

manometer, electrolyte reservoir, and a circulation pump (Fig. 1).

The electrolyser, in the form of a vertical flow-through channel, was provided with a poly(methylmethacrylate) frame, the plate electrodes were 4 mm apart and the channel width was 80 mm. The electrode dimensions were 88 mm × 118 mm × 1 mm and their active surface area was 80 mm × 118 mm. The anode was made of titanium sheet covered with a layer of 30 mol % RuO_2 and 70 mol % TiO_2, the cathode was made of steel (CSN 17241, 18% Cr, 8% Ni). The channel cross-section was 4 mm × 80 mm.

The electric current was supplied by three controllable stabilized d.c. current sources RFT 3216, 20A, 30V, (Statron, Germany) connected in parallel and fed from the a.c. mains. The current value was read on two ammeters ML 20, 30A (Metra Blansko, Czech Republic) of 0.2% accuracy, connected in parallel. The terminal voltage of the electrolyser was measured with a digital voltmeter DM 2022S (Solartron, UK).

The electrolyte was pumped through the Venturi tube provided with a U-manometer into the lower part of the electrolyser. The solution flowed from the upper part of the electrolyser together with the evolved gases (H_2, O_2, and traces of Cl_2) into the gas separator and through the spiral cooler back into the reservoir. The temperature of the electrolyte was controlled by means of the contact thermometer, which switched the cooling circuit of the thermostat on and off. The gas separated from the electrolyte was fed into an Orsat device for analysis. The electrolyte consisted of 10 dm^3 of a solution of NaCl.

A pH meter of type OP 204/1 (Radelkis, Budapest) was used for pH measurements using a glass electrode of type G202C (Radiometer Copenhagen) and Radelkis calomel reference electrode of type OP-0830P.

3.2. *Measurement*

Electrolysis was carried out until the charge passed reached at least 32 kC dm^{-3}. Samples of the electrolyte were taken at regular intervals. The hypochlorite content was determined according to Penot (by retitrating the excess sodium arsenite with iodine and using starch as indicator). The content of chlorate was determined manganometrically according to Zimmermann and Reinhardt (by retitration of the excess iron sulphate with $KMnO_4$.) At the same time, a gas sample was taken and then analysed in the Orsat apparatus. Chlorine was absorbed in 25% KOH and oxygen in an alkaline pyrogallol solution. The electrolyser voltage and solution pH were measured before and during the electrolysis. Experiments were made at current densities of 1059.3, 1652.5, 3178.0 and 4237.3 A m^{-2}. The initial concentrations of NaCl were 15 and 30 g dm^{-3}, the rate of flow of electrolyte through the electrolyser was 0.086 dm^3 s^{-1}, the Reynolds number was 2054–2100 and the temperature was 20° C. One experiment lasted for 3–9 h; the electrolysis continued until the charge passed was at least 32 kC dm^{-3}.

Table 1. Experimental results obtained for the electrolysis of dilute solutions of NaCl at pH ~ 6–9, temperature 25 ± 1° C, batch system with a flow-through electrolyser and electrolyte volume 10 dm^3

	Initial NaCl concentration/g dm^{-3}					
	15	15	30	30	30	30
Current density/A dm^{-2}	1059	4237	1059	1653	3178	4237
Cell voltage/V initial	4.85	11.3	4.05	4.55	6.75	8.00
Cell voltage/V final	5.05	11.5	4.35	4.65	7.05	8.30
End concentration of NaClO for QV^{-1} = 32 kC dm^{-3}/g dm^{-3}	7.067	7.336	7.760	8.593	9.069	9.144
End concentration of $NaClO_3$ for QV^{-1} = 32 kC dm^{-3}/g dm^{-3}	0.316	0.787	0.167	0.199	0.304	0.311
Y_{ClO^-} for QV^{-1} = 32 kC dm^{-3}/%	57.26	59.44	62.89	69.62	73.61	74.15
$y_{ClO^-} + y_{ClO_3^-}$ (C_{NaClO} = 7 g dm^{-3})/%	46.57	59.11	54.93	65.56	74.97	76.08
y_r (C_{NaClO} = 7 g dm^{-3})/%	30.41	13.49	31.47	21.93	13.46	15.63

Table 2. Time dependences of current yields and concentrations of ClO^- and ClO_3^- for the experiment with $C_{NaCl} = 30\,g\,dm^{-3}$ and $j = 1059\,A\,dm^{-2}$, electrolyte volume $V = 10\,dm^3$

	Time/s										
	2700	5400	8100	10 800	13 500	16 200	18 900	21 600	24 300	27 000	29 700	32 400
Charge passed/kC dm^{-3}	2.70	5.40	8.11	10.82	13.53	16.24	18.96	21.68	24.40	27.13	29.86	32.59
C_{NaClO}/g dm^{-3}	0.868	1.696	2.485	3.238	3.958	4.647	5.265	5.843	6.390	6.907	7.396	7.860
C_{NaClO_3}/g dm^{-3}	0.0	0.0	0.0	0.0	0.0	0.0	0.020	0.046	0.074	0.106	0.140	0.175
Y_{ClO^-}/%	83.38	81.36	79.44	77.61	75.85	74.17	71.98	69.87	67.88	66.00	64.22	62.53
$Y_{ClO_3^-}$/%	0.00	0.00	0.00	0.00	0.00	0.00	0.58	1.15	1.66	2.10	2.54	2.92
y_{ClO^-}/%	83.38	79.35	75.60	72.10	68.83	65.78	58.84	55.18	51.96	49.07	46.40	43.94
$y_{ClO_3^-}$/%	0.00	0.00	0.00	0.00	0.00	0.00	4.08	5.12	5.75	6.29	6.72	7.08
y_r/%	6.34	9.88	13.16	16.25	19.13	21.81	24.33	26.70	28.91	31.00	32.96	34.81

4. Results

4.1. *Experimentally determined current yields*

The initial pH value was always around 6; during the first several minutes of electrolysis it rose to about 9.0–9.2, and during another 20 min it attained a steady value of 9.55 ± 0.15. This suggests that, initially, a minute amount of chlorine escapes with the evolved hydrogen and oxygen, resulting in a pH change. The quantity of chlorine lost is very small, since no chlorine was detected by gas analysis (with an accuracy of 0.1%). In the alkalized solution (pH 9.2–9.5), chlorine is practically completely absorbed, so that the pH becomes constant.

The experiments suggest that the concentration of NaClO (i.e. the integral current yield) at a charge of 32 kC dm^{-3} increases both with the current density and initial concentration of NaCl, as can be seen from Table 1. The final concentrations of NaClO of 7–9 g dm^{-3} are sufficient for practical application in the disinfection of water.

The final concentration of $NaClO_3$ was 0.3–0.8 g dm^{-3} at a charge of 32 kC dm^{-3}; the concentration increased with current density and with decreasing initial concentration of NaCl. From the disinfection point of view the concentration of chlorate in the solution for water treatment is low (Table 1).

The current yield with respect to cathodic reduction of NaClO was 13–32%; it decreased with increasing total current density and was directly proportional to the concentration of NaClO (Table 2). The reduction of hypochlorite is slightly enhanced with increasing input concentration of NaCl (Table 1).

4.2. *Theoretical current yield for reduction of hypochlorite*

The calculations were based on Equations 25–29 and Equations 39–41 and the thickness of the Nernst diffusion layer was calculated from Equations 10, 11, 15(a) and 19. The concentration of chlorate was set to zero. The diffusion coefficient of ClO^- ions is given in the literature [14–17] with a scatter of about 20%; the value given by Chao was used [15] (0.89×10^{-9} m^2 s^{-1} for 20° C and 0.5 M NaCl). The diffusion coefficients of other ions were estimated from the values for NaCl, KCl, KOH and NaOH [19] on the assumption that the ratio of the values for K^+ and Cl^- ions is equal to 1.01 [19] and is independent of temperature and the presence of other

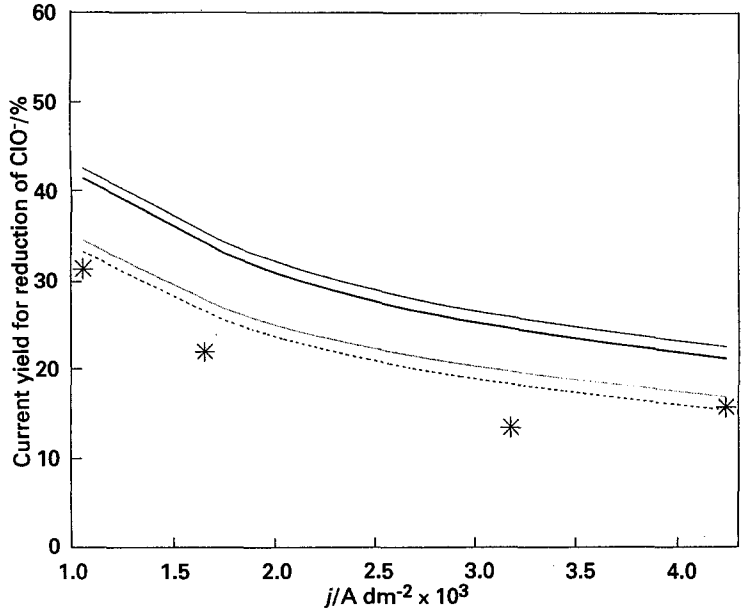

Fig. 2. Dependence of the current yield for reduction of ClO^- ions on the total current density, $T = 20°$ C, $Re = 2054$, pH 9.5, $C_{NaClO} = 7\,g\,dm^{-3}$, $C_{NaCl} = 30\,g\,dm^{-3}$, $d_B = 0.04$ mm. Key: (*) experiments; θ: (—) 0.787 diff., (—) 0.787 diff. + mig., (· · ·) 0.897 diff., (- - -) 0.897 diff. + mig.

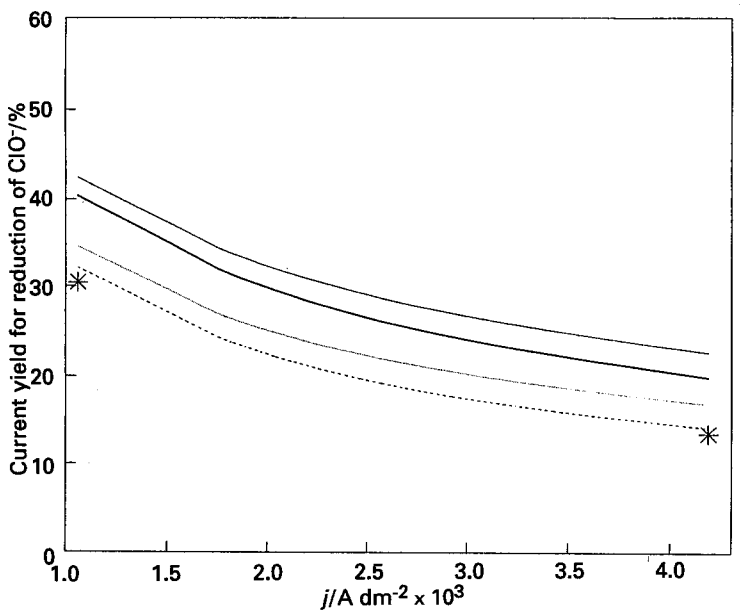

Fig. 3. Dependence of the current yield for reduction of ClO^- ions on the total current density, $T = 20°$ C, $Re = 2100$, pH 9.5, $C_{NaClO} = 7\,g\,dm^{-3}$, $C_{NaCl} = 15\,g\,dm^{-3}$, $d_B = 0.04$ mm. Key: as in Fig. 2.

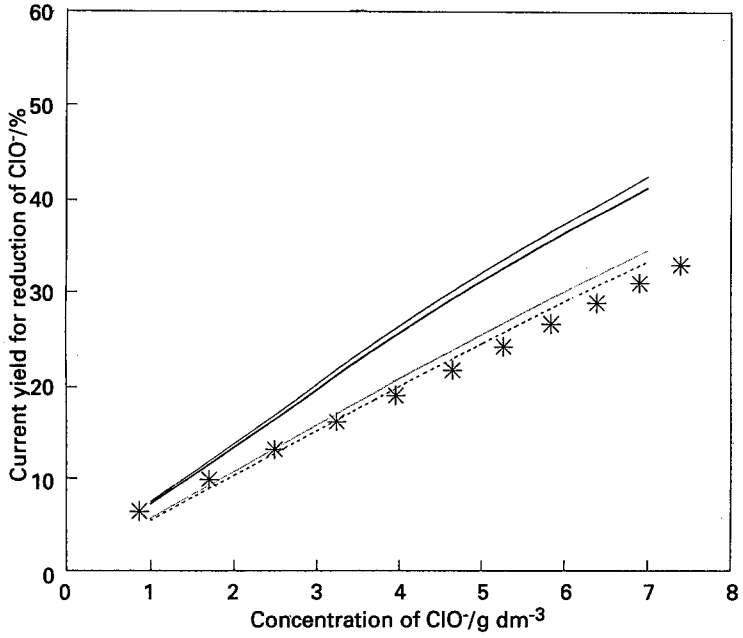

Fig. 4. Dependence of the current yield for reduction of ClO^- ions on concentration for $j = 1059\,A\,m^{-2}$, $T = 20°$ C, $Re = 2154$, pH 9.5, $C_{NaCl} = 30\,g\,dm^{-3}$, $d_B = 0.04$ mm. Key: as in Fig. 2.

salts (NaCl and NaClO). Viscosities of NaCl solutions were taken from [20].

The current yield for ClO^- reduction was calculated both without and with regard to migration ($M = 1$ and $M < 1$). The critical point was, besides estimation of the diffusion coefficient of NaClO, estimation of the coverage of the electrode with hydrogen bubbles occurring in Equations 15(a) and 17. The dependence of the current yield for reduction of ClO^- ions on the total current density for two initial NaCl concentrations is shown in Figs 2 and 3 and the dependence of current yields for ClO^- ion reduction on concentration for $j = 1059\,A\,dm^{-2}$ is demonstrated in Fig. 4. With the use of the recommended bubble diameter $d_B = 0.040$ mm [5] and coverage $\theta = 0.25$, the flux of hypochlorite to the cathode surface is appreciably greater than that corresponding to the flux calculated from the measured reduction

Table 3. Current yield (differential) for reduction of ClO^-. Experimental and calculated current yields for $d_B = 0.04$ mm [1]

No. of exp. according to [1]	*Re*	$y_{ClO^-,r}$ *(exp)*	$y_{ClO^-,r}$ *(calculated, this study)*			
			Only diff.	*Diff. + migr.*	*Only diff.*	*Diff. + migr.*
			$\theta = 0.787$		$\theta = 0.897$	
9	1484	49.48	56.88	53.15	46.64	42.66
10	3180	64.35	60.85	59.42	56.14	54.62
16a	2081	55.44	65.59	65.07	55.76	55.17
17	1890	54.46	55.67	52.96	45.70	41.94

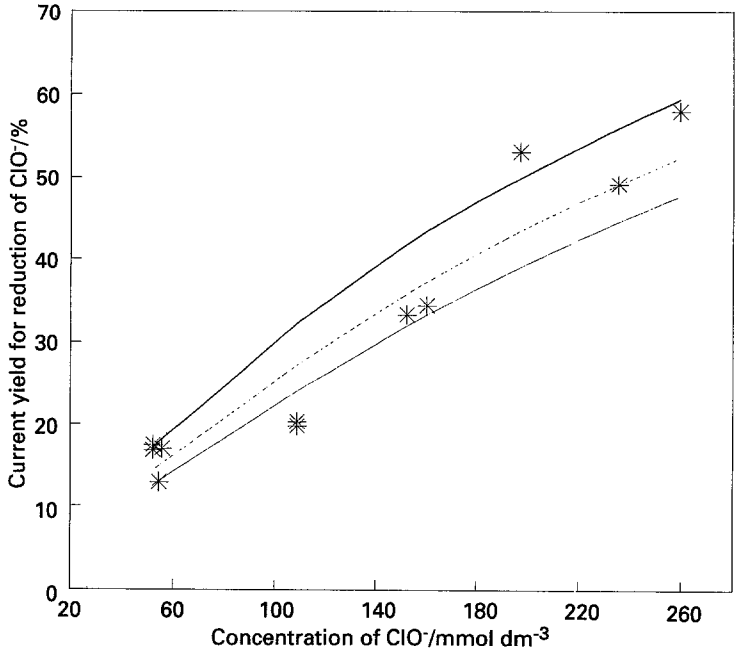

Fig. 5. Dependence of the current yield for reduction of ClO^- ions on concentration for $j = 1450\,A\,m^{-2}$. Free convection, $C_{NaCl} = 150\,g\,dm^{-3}$, $d_B = 0.04\,mm$. Calculated from the data taken from [3]. Key: (*) experiments; θ: (—) 0.897, (- - -) 0.932 and (—) 0.949.

rate of hypochlorite. The best agreement with the measured values was obtained by using a coverage, θ, of 0.897 and a bubble diameter, d_B, of 0.040 mm.

Migration of ClO^- ions to the anode caused diminution of their flux to the cathode. The current yield for reduction of NaClO calculated with regard to migration is by 1–2% lower than that with neglection of migration. The migration factor, M, decreases with increasing current density or decreasing concentration of NaCl. This is illustrated in Figs 2–4.

To compare the present data with those in the literature, the current yields were calculated for the conditions given there. The experimental and calculated current yields for reduction of ClO^- for two coverages θ (calculated for data taken from [1]) are expressed in Table 3. The data of Robertson *et al.* [1] were well approximated by using $\theta = 0.787$ and $d_B = 0.04$ mm. The effect of migration was more pronounced because of the higher concentration of NaClO (about 15 g NaClO dm^{-3}) than in the present experiments.

The dependence of current yields for ClO^- ion reduction (calculated for data taken from [3]) on concentration for $j = 1450$–$20\,400\,A\,m^{-2}$ are shown in Figs 5–9. The data of Hammar and Wranglen [3] are best approximated by using the coverage $\theta = 0.925$ and $d_B = 0.04$ mm. Experiments [3] were performed with natural convection due to the rising effect of bubbles. Here, the concentration of NaCl was as high as $150\,g\,dm^{-3}$ so that the effect of migration was to lower the current yield for reduction of ClO^- by as little as 0.5%.

The dependence of $Sh_B[\theta_1^{0.25}(1-\theta_1^{0.5})^{0.5}]/Sc^{0.487}[\theta^{0.25}(1-\theta^{0.5})^{0.5}]$ on Re_B for various coverages

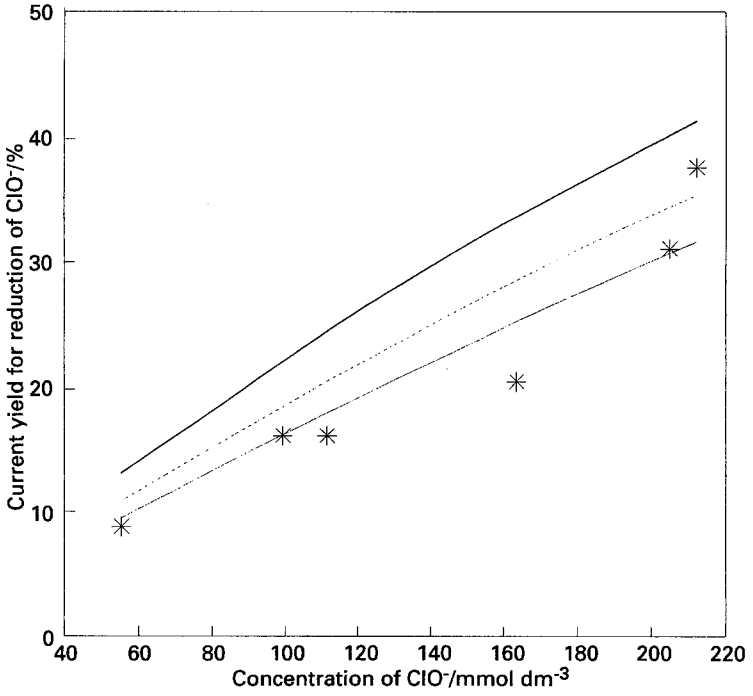

Fig. 6. Dependence of the current yield for reduction of ClO^- ions on concentration for $j = 2900\,A\,m^{-2}$. Further description and key: see Fig. 5.

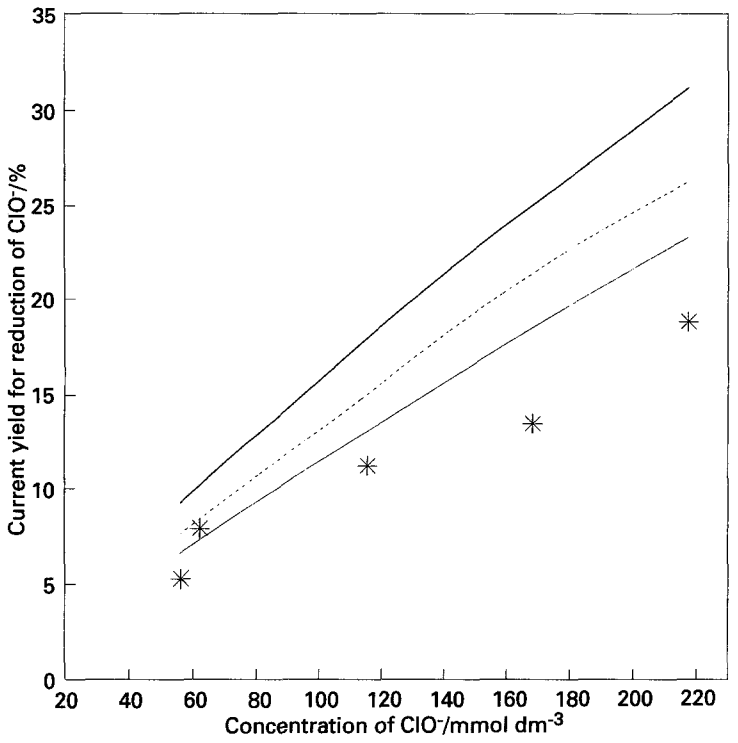

Fig. 7. Dependence of the current yield for reduction of ClO^- ions on concentration for $j = 6300\,A\,m^{-2}$. Further description and key: see Fig. 5.

for the present results is shown in Fig. 10. The Sherwood number, Sh_B, was calculated from experimental measured limiting current densities for the reduction of ClO^- ions ($j_{c,lim}$). Also the Reynolds number for bubbles (Re_B) was calculated from the experimental current densities ($j - j_{c,lim}$). This means that both values (Sh_B and Re_B in Fig. 10) are not exactly valid for the case of convection due to bubble evolution. Comparing the δ_B and δ_C values the forced convection changes the Sh_B values by 10–15% for all Reynolds numbers (Re). The dependence of $Sh_B[\theta_1^{0.25}(1-\theta_1^{0.5})^{0.5}]/Sc^{0.487}[\theta^{0.25}(1-\theta^{0.5})^{0.5}]$ on Re_B for various coverages (calculated for data taken from [3]) is shown in Fig. 11. It is apparent that there is an appreciable shift of data with coverage, θ.

Robertson *et al.* [1] used a higher electrolyte flow rate compared to the present experiments. It was found here that $\theta = 0.787$ is acceptable for Equation 15(a). Hammar and Wranglen [3] used natural convection; for that case we found $\theta = 0.949$ for Equation 15(a) (see Fig. 11). The present experiments with Reynolds numbers between 2054–2100 represents an intermediate between the two and we found that $\theta = 0.897$ is appropriate for Equation 15(a) (see Fig. 10). Thus, the coverage of the electrode with bubbles, θ, increases with decreasing rate of flow along the electrode. The finding that θ increases as the flow velocity decreases was also made by Silen [21].

The change of θ and d_B with current density was studied by Vogt [9–11, 22–25] and the following

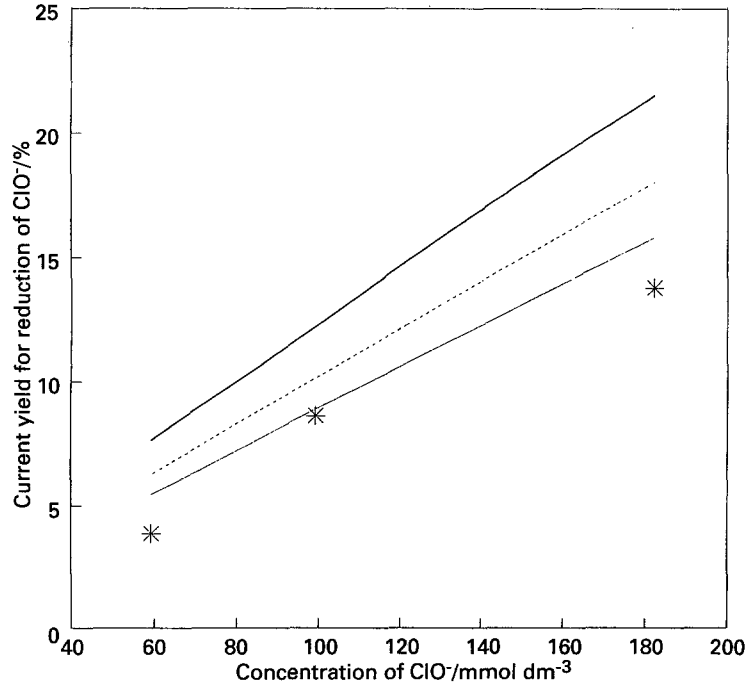

Fig. 8. Dependence of the current yield for reduction of ClO^- ions on concentration for $j = 10\,500\,A\,m^{-2}$. Further description and key: see Fig. 5.

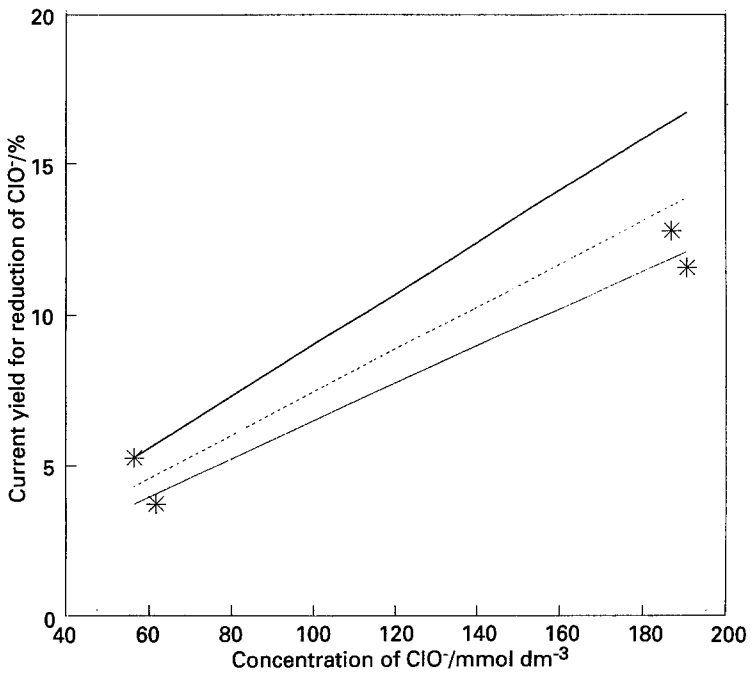

Fig. 9. Dependence of the current yield for reduction of ClO^- ions on concentration for $j = 20\,400\ A\ m^{-2}$. Further description and key see Fig. 5.

correlation was recommended for hydrogen evolution at platinum electrodes [11]:

$$\Theta = 0.8\left(\frac{j}{j_{cr}}\right)^{0.25} \tag{49}$$

where j_{cr} represents a critical current density depending on the stirring of the electrolyte [26, 27]. It has been found, that d_B depends on the coverage θ (also called the shielding number) and may be estimated from [28]:

$$d_B = \left(50^2 + \left(\frac{10}{\Theta}\right)^2\right)^{0.5} \tag{50}$$

where d_B is in micrometres. Because the experimental conditions for the system studied here (pH ~ 6–9) are different from experimental conditions used for the derivation of Equations 49 and 50 these equations were not used for more detailed analysis.

5. Conclusion

The separation of boundary conditions necessary for the solution of the transport equation for ionic species OH^-, Cl^-, ClO^-, ClO_3^- and Na^+ in the Nernst boundary layer at the cathode was performed and the migration correction for the ClO^- flux was calculated theoretically. In 1.5% NaCl, the migration correction causes lowering of the reduction yield by only about 2%. The coverage of the cathode with

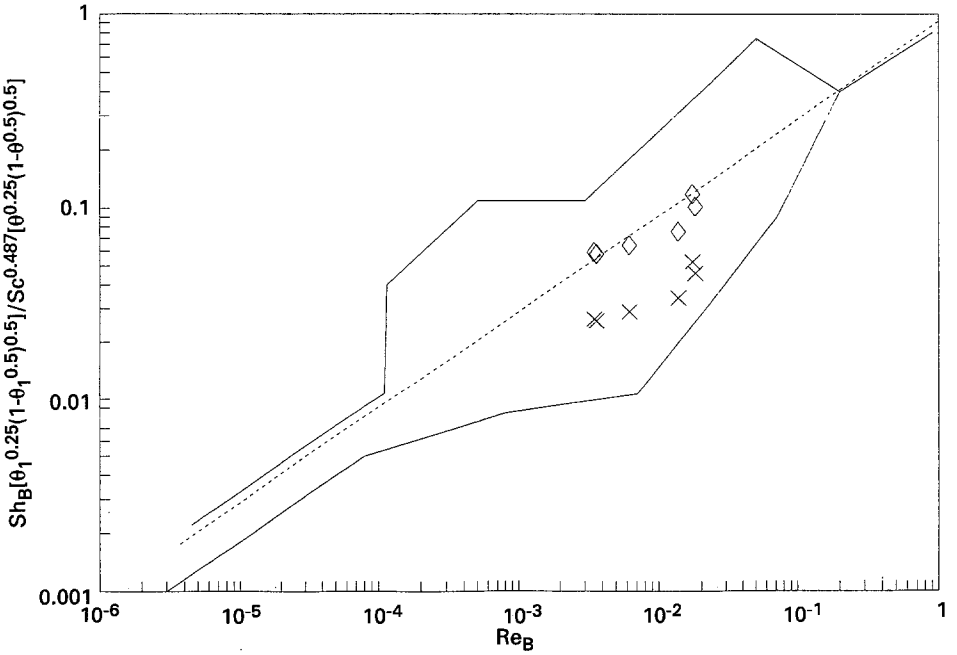

Fig. 10. Dependence of $Sh_B[\theta_1^{0.25}(1-\theta_1^{0.5})^{0.5}]/Sc^{0.487}[\theta^{0.25}(1-\theta^{0.5})^{0.5}]$ on Re_B for various coverages θ (present results). Solid line indicates scatter of experimental data in Equation 15. (Cf. Fig. 4 in [1].) Key: (- - - -) Equation 15, (×) $\theta = 0.250$ and (◇) $\theta = 0.897$.

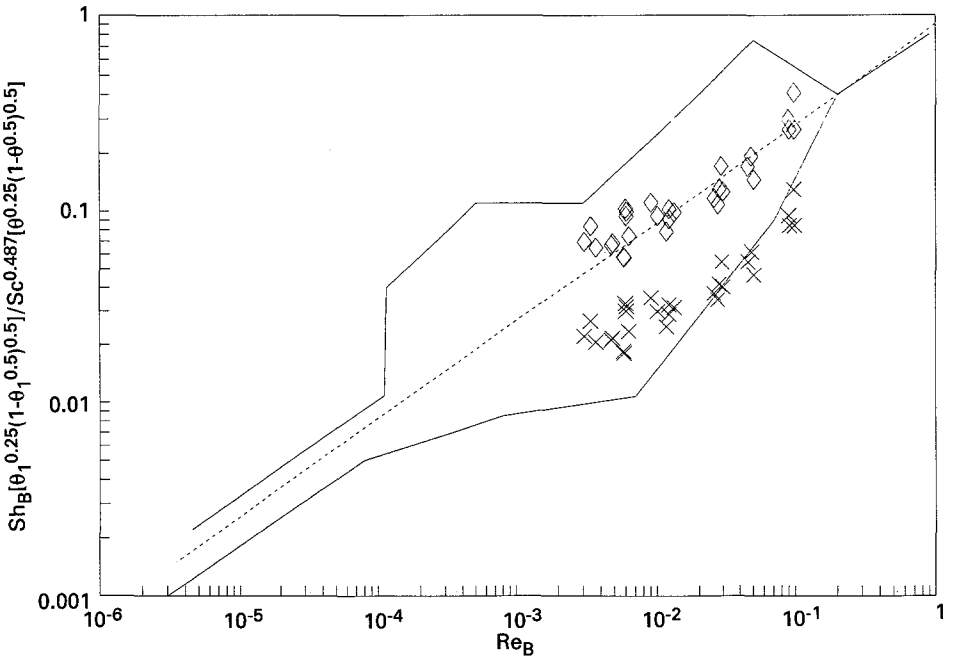

Fig. 11. Dependence of $Sh_B[\theta_1^{0.25}(1-\theta_1^{0.5})^{0.5}]/Sc^{0.487}[\theta^{0.25}(1-\theta^{0.5})^{0.5}]$ on Re_B for various coverages θ (calculated for the data taken from [3]). For the further description see Fig. 10. Key: (- - - -) Equation 15, (×) $\theta = 0.250$ and (◇) $\theta = 0.949$.

hydrogen bubbles in NaCl solutions is in the range 0.787–0.949 assuming a bubble diameter of 0.04 mm at current densities of 1059–20 400 A m^{-2}. The least coverage ($\theta = 0.787$) corresponds to a high electrolyte flow rate at the cathode, and the highest coverage ($\theta = 0.949$) corresponds to natural convection caused by bubble rise in the cell. Results of calculations in the present work confirm that the scatter of experimental data in Fig. 4 [5] are connected with the change of bubble diameter d_B and the coverage θ with total applied current density.

References

[1] P. M. Robertson, W. Gnehm and L. Ponto, *J. Appl. Electrochem.* **13** (1983) 307.
[2] N. Krstajic, V. Nakic and M. Spasojevic, *J. Appl. Electrochem.* **21** (1991) 637.
[3] L. Hammar and J. Wranglen, *Electrochim. Acta* **9** (1964) 1.
[4] J. E. Bennett, *Chem. Eng. Prog.* **70** (1974) 60.
[5] K. Stephan and H. Vogt, *Electrochim. Acta* **24** (1979) 11.
[6] H. Vogt, *ibid.* **23** (1978) 203.
[7] K. L. Hardee and L. K. Mitchell, *J. Electrochem. Soc.* **136** (1989) 3314.
[8] I. Rousar, K. Micka and A. Kimla, 'Electrochemical Engineering II', Academia Praha, Elsevier Amsterdam (1986) pp. 23 and 34.
[9] H. Vogt, *Electrochim. Acta* **25** (1980) 527.
[10] *Idem, Electrochem. Acta* **38** (1993) 1427.
[11] J. Newman, *I&EC Fundamentals* **5** (1966) 525.
[12] O. Wein, *Coll. Czech. Chem. Comm.* **33** (1988) 697.
[13] O. Schwarzer and R. Landsberg, *J. Electroanal. Chem.* **19** (1968) 391.
[14] M. S. Chao, *J. Electrochem. Soc.* **115** (1968) 1172.
[15] J. A. Harrison and Z. A. Kahn, *J. Electroanal. Chem.* **30** (1971) 87.
[16] L. R. Czarnetzki and L. J. J. Janssen, *Electrochim. Acta* **33** (1988) 361.
[17] Landolt-Börnstein, 'Zahlenwerte und Funktionen', vol. II/5a, Springer Verlag, Berlin, (1969) p. 614.
[18] P. Pitner and coworkers, 'Hydrochemical Tables' (in Czech), SNTL, (1987) p. 118.
[19] J. Dykyj and coworkers, 'Physiochemical Tables I' (in Czech), SNTL Praha, (1953) p. 389.
[20] C. W. M. P. Silen, PhD thesis, Eidhoven (1983).
[21] H. Vogt, *Electrochim. Acta* **29** (1984) 167.
[22] H. Vogt, *J. Electrochem. Soc.* **137** (1990) 1179.
[23] *Idem, J. Appl. Electrochem.* **19** (1989) 713.
[24] *Idem, Electrochim. Acta* **38** (1993) 1421.
[25] *Idem, Int. J. Heat Mass Transfer* **36** (1993) 4115.
[26] B. Mazza, P. Pedeferri, R. Piontelli and A. Tognoni, *Electrochim. Metal* **2** (1967) 385.
[27] J. O'M. Bockris and A. M. Azzam, *Trans. Faraday Soc.* **48** (1952) 145.
[28] H. Vogt, *Electrochim. Acta* **34** (1989) 1429.